Investigation of q-dependent dynamical heterogeneity in a colloidal gel by x-ray photon correlation spectroscopy

V. Trappe,[1] E. Pitard,[2] L. Ramos,[2] A. Robert,[3,*] H. Bissig,[1] and L. Cipelletti[2,†]

[1]*Departement de Physique, Université de Fribourg, Chemin du Musée 3, 1700 Fribourg, Switzerland*

[2]*Laboratoire des Colloïdes, Verres et Nanomatériaux (UMR CNRS-UM2 5587), CC26, Université Montpellier 2, 34095 Montpellier Cedex 5, France*

[3]*European Synchrotron Radiation Facility—6 rue Jules Horowitz BP 220, F-38043 Grenoble Cedex 9, France*

We use time-resolved x-ray photon correlation spectroscopy to investigate the slow dynamics of colloidal gels made of moderately attractive carbon black particles. We show that the slow dynamics is temporally heterogeneous and quantify its fluctuations by measuring the variance χ of the instantaneous intensity correlation function. The amplitude of dynamical fluctuations has a nonmonotonic dependence on scattering vector q, in stark contrast with recent experiments on strongly attractive colloidal gels [Duri and Cipelletti, Europhys. Lett. **76**, 972 (2006)]. We propose a simple scaling argument for the q-dependence of fluctuations in glassy systems that rationalizes these findings.

PACS number(s): 82.70.Dd, 64.70.Pf, 82.70.Gg

I. INTRODUCTION

Understanding the dramatic slowing down of the dynamics in systems undergoing a glass transition is one of the key problems in condensed matter and statistical physics [1]. In recent years, research efforts have focused on the role of dynamical heterogeneity: as the glass transition is approached, the dynamics becomes increasingly correlated in space, since rearrangements are possible only through the cooperative motion of "clusters" of particles [2–4]. This cooperativity leads to strong temporal fluctuations of the dynamics. Indeed, because of dynamical correlations, the number of statistically independent objects in the system becomes smaller than the number of particles, leading to enhanced fluctuations.

Numerical simulations have tested these features on a wide variety of systems [4]. Experimental work, by contrast, is much more scarce, because probing the dynamics with the spatial and temporal resolution needed to highlight their heterogeneous nature is an arduous task, especially for molecular glass formers [2,3]. The slow dynamics of colloidal systems, foams, and granular materials [5] share intriguing similarities with those of glass formers, including dynamical heterogeneities. These are experimentally more accessible than in molecular systems, since the relevant time and length scales are larger. Various techniques have been used to characterize them, from direct space measurements [6–8] to scattering methods that probe the temporal fluctuations of the intensity correlation function [9–12].

Valuable information on the physical origin of the average dynamics is generally obtained by studying its length scale dependence, e.g., the dependence of the intensity correlation function on the magnitude of the scattering vector q in scattering experiments. Similarly, one expects to gain a better understanding of dynamical heterogeneities by analyzing their behavior at different q's. Unfortunately, experimental and numerical or theoretical determinations of dynamical fluctuations as a function of q are still very scarce [7,12–17], leaving this issue an open question.

In this paper, we investigate dynamical fluctuations in colloidal gels made of moderately attractive carbon black (CB) particles, to which a dispersant is added to control the strength of the (attractive) interparticle interactions. We apply, to our knowledge for the first time, time-resolved scattering methods to x-ray photon correlation spectroscopy (XPCS), thereby demonstrating that the dynamics of the CB gels are temporally heterogeneous. Dynamical fluctuations are quantified by means of a q-dependent dynamical susceptibility χ, similar to the dynamical susceptibility χ_4 studied in simulations [16]. Surprisingly, χ is found to initially increase with q, but eventually to decrease at large scattering vectors. This nonmonotonic behavior is in contrast with recent low-q measurements on diluted, strongly attractive colloidal gels [12], where dynamical fluctuations increased linearly with q over one decade in scattering vector. We propose a simple scaling argument for the q dependence of dynamical fluctuations in glassy systems, which reconciles these contrasting findings and rationalizes previously published data for granular media and glass formers [7,13–16].

The paper is organized as follows. In Sec. II we present and characterize our experimental system and introduce shortly the time-resolved XPCS technique. Section III reports both the average dynamics of the CB gels and its temporally fluctuations. Our results are discussed in Sec. IV, where a simple scaling argument for the length scale dependence of the dynamical susceptibility is introduced.

II. MATERIALS AND METHODS

A. Sample preparation and characterization

Particle size and morphology. Our gels are made of CB particles of average radius $\bar{R}=180$ nm, suspended in mineral

*Present address: Stanford Linear Accelerator Center, 2575 Sand Hill Road, Menlo Park, California 94025, USA.

†lucacip@lcvn.univ-montp2.fr

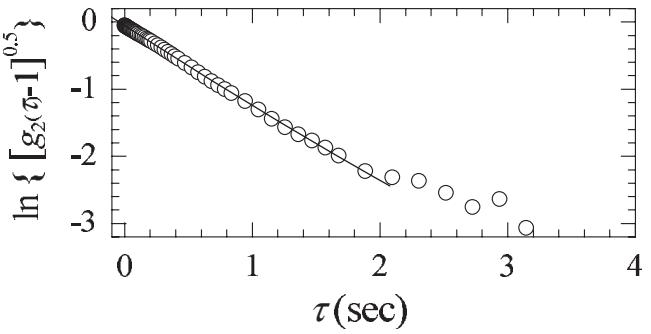

FIG. 1. Second-order cumulant fit (line) of the intensity correlation function (open circles) measured by dynamic light scattering at $q=6.01\ \mu m^{-1}$ for a diluted suspension of CB particles.

oil at an effective volume fraction $\varphi \approx 6\%$, as determined by viscosity measurements (see below). The particles have a conveniently high scattering cross section for x rays. They are fractal aggregates made of permanently fused primary particles (fractal dimension $d_f=2.2\pm0.1$) [18]. The diameter of the primary particles ranges from 20 to 40 nm, as determined by electron microscopy. However, the smallest units in our samples are effectively the CB particles themselves and not the primary particles, since the CB particles can not be broken, neither by thermal fluctuations, nor by adding a dispersant or by applying a large shear, e.g., during rheology tests or sonication. The size and polydispersity of the CB particles were determined by applying the cumulant analysis described in Ref. [19] to intensity correlation functions measured by dynamic light scattering (DLS) at $q=6.01\ \mu m^{-1}$ (scattering angle $\theta=20°$). A very diluted ($\varphi \approx 2\times10^{-6}$) and fully dispersed sample of CB particles in mineral oil was prepared for the DLS measurements. For spherical, monodisperse particles, one expects the intensity correlation function g_2-1 to relax exponentially; deviations due to shape and/or size polydispersity may be quantified by the ratio κ_2/κ_1^2, where κ_i is the ith coefficient of a cumulant expansion $\ln\{[g_2(\tau)-1]^{0.5}\}=\kappa_0-\kappa_1\tau+\kappa_2\tau^2/2+\cdots$ [19].

Figure 1 shows $\ln\{[g_2(\tau)-1]^{0.5}\}$ vs τ for our DLS measurements: the data are very close to a straight line, indicating a nearly exponential decay and thus suggesting that the sample polydispersity must be moderate. By generalizing the arguments of Ref. [19] to particles with a fractal morphology, one finds that in the low-q limit ($qR \lesssim 1$) the first two cumulants are related to the average translational diffusion coefficient $\bar{D}$ and its relative variance $\sigma_D^2=(\overline{D^2}/\bar{D}^2-1)$, by the following expressions:

$$\kappa_1 = \bar{D}q^2, \tag{1}$$

$$\kappa_2 = \sigma_D^2(\bar{D}q^2)^2/2, \tag{2}$$

with $\bar{D}=k_BT/(6\pi\eta R_{app})$, $R_{app}=\overline{R^{2d_f}}/\overline{R^{2d_f-1}}$, T the temperature and k_B the Boltzman's constant. Here, $\overline{R^n}=\int dRP(R)R^n$ is the nth moment of the normalized number distribution of particle radii $P(R)$. For the data shown in Fig. 1, we find $\sigma_D^2=2\kappa_2/\kappa_1^2=0.047$, confirming that the polydispersity is moderate. The average particle radius and its relative variance $\sigma_R^2=(\overline{R^2}/\bar{R}^2-1)$, may be obtained from σ_D^2 and R_{app} provided that $P(R)$ is known. Since for moderate polydispersity the exact shape of $P(R)$ has little influence on the final result, we choose a generalized exponential (or Schulz) distribution, for which calculations can be performed analytically [19]. By taking for simplicity $d_f=2$ (very close to the value 2.2 of our particles), one finds

$$R_{app} = \overline{R^4}/\overline{R^3} = \bar{R}(1+3\sigma_R^2), \tag{3}$$

$$\sigma_D^2 = \frac{\overline{R^2R^4}}{\overline{R^3}^2} - 1 = \frac{1+3\sigma_R^2}{1+2\sigma_R^2} - 1, \tag{4}$$

yielding for our CB particles $\bar{R}=180$ nm and $\sigma_R=0.23$.

Determination of the volume fraction The particle concentration of the two CB gels studied here is 2% w/w. The effective volume fraction corresponding to this weight fraction was determined by measuring the viscosity of a suspension where the CB particles were fully dispersed (1.6% w/w dispersant). The effective hydrodynamic volume fraction φ is estimated using [20] $\eta_\infty/\mu=(1-\varphi/0.71)^{-2}$, where μ is the shear-independent viscosity of the mineral oil and η_∞ is the high shear rate viscosity of the suspension. The value $\varphi \approx 6\%$ thus obtained was found to be consistent with that obtained by measuring the low-shear viscosity of the suspension η_0 and using [20] $\eta_0/\mu=(1-\varphi/0.63)^{-2}$.

Estimate of the depth of the particle-particle interaction potential. The attraction between CB particles is controlled by the amount of added dispersant. The depth of the well of the particle-particle interaction potential U may be estimated by studying the mechanical response of the CB gels. As discussed in Refs. [21,22], the relaxation spectrum (as measured by oscillatory rheology) of CB suspensions and its dependence on volume fraction is essentially identical to that obtained for model systems of nearly monodisperse spherical particles that interact via a short-ranged potential induced by the depletion mechanism. Therefore, we use the nonequilibrium state diagram of the depletion systems with known depth of the interaction potential to evaluate U for our CB gels. The diagram is shown in Fig. 3 of Ref. [21]: the control parameters are φ and U; a line $U=U_c(\varphi)$ separates the systems with solidlike mechanical behavior (upper part of the diagram) to those with a liquidlike behavior (lower part). For the CB gel with 0.2% dispersant, we find that the elastic modulus is very low ($G_p=9\times10^{-4}$ Pa), which indicates that this system corresponds to a state close to the fluid-solid boundary. Figure 3 of Ref. [21] indicates that for short ranged potentials the boundary corresponds to $U=U_c \approx 12k_BT$ at $\varphi=6\%$. Thus, we assign $U\approx12k_BT$ to the CB gel at $\varphi=6\%$ and with 0.2% dispersant.

For the CB system with 0% dispersant, we take advantage of the dependence of the elastic modulus on dispersant concentration, which was found to exhibit a critical-like behavior $G_p=G_0(U/U_c-1)^\nu$, with $\nu=3.9$ and $G_0\approx1$ Pa [18]. We measure $G_p=4.5$ Pa for the CB gel without dispersant, yielding $U\approx2.5U_c\approx30\ k_BT$.

Sample preparation. The CB suspensions are prepared from a stock suspension of 4% w/w carbon black (Cabot

Vulcan XC72) in light mineral oil (Aldrich). The stock solution is made by first mixing the carbon black powder into the mineral oil using a standard household mixer. Subsequently, it is thoroughly sonicated for 1 hour using an ultrasound device (Hielscher UP200H) operating at a power of 120 W and a frequency of 24 kHz. To avoid overheating, the suspension is placed in an ice bath and sonication is run in cycles of 1 s. The stock solution is then left to equilibrate for 2 days, before it is used to prepare the final samples. Before diluting the sample to a final concentration of 2% w/w CB (corresponding to $\varphi \approx 6\%$), the stock suspension is again thoroughly mixed; the final samples are then prepared by adding either pure mineral oil or a solution of dispersant in mineral oil; they are mixed and left to equilibrate for 2 days. Prior to the XPCS experiments, the samples are again thoroughly mixed and subsequently injected in a 1 mm (inner diameter) cylindrical capillary. The capillary is sealed and placed in a water bath in which we introduce our ultrasound device, thereby submitting the sample to a final indirect sonication step (120 W and 24 kHz) for about half an hour. We define the age of sample t_w as being the time elapsed since this final sonication step. Note that sonication breaks up any aggregates that may have been formed between the CB particles, without affecting the integrity of the CB particles themselves.

B. Time-resolved XPCS measurements

Average dynamics. The dynamics of the CB gels are investigated by means of XPCS performed at the ID10 Troika beamline at the European Synchrotron Radiation Facility (ESRF), with x rays of wavelength $\lambda = 1.55$ Å. The scattering volume has a cylindrical shape, with diameter 12 μm and length 1 mm (along the horizontal direction), defined by the beam size and the capillary diameter, respectively. The scattered intensity is recorded by a charge-coupled device (CCD) camera, covering about one decade in scattering vector $15\ \mu\text{m}^{-1} \lesssim q \lesssim 150\ \mu\text{m}^{-1}$, corresponding to distances comparable to or smaller than the CB particle size. XPCS measurements start at age $t_w = 2$ min: we find that the dynamics initially slows down, as observed for many glassy systems [5], but that after a few hours a stationary state is attained. All measurements presented in this work start at $t_w = 5$ hours, well in the stationary regime, and last typically up to 3 h. Mechanical and beam instabilities are a concern when measuring very slow dynamics, especially in XPCS experiments. By using a static scatterer (Vycor glass), we have checked that the setup was stable up to $\tau \approx 3000$ s, longer than the relevant time scales in our experiments.

In order to measure the average dynamics and its fluctuations, we use the time-resolved correlation (TRC) method [9]. The instantaneous degree of correlation between x-ray photons scattered at time t and $t+\tau$ is measured according to $c_I(q,t,\tau) = \langle I_p(t) I_p(t+\tau)\rangle_q / (\langle I_p(t)\rangle_q \langle I_p(t+\tau)\rangle_q) - 1$, where $I_p(t)$ is the scattered intensity at pixel p and time t and $\langle \cdots \rangle_q$ is an average over a ring of pixels corresponding to approximately the same magnitude of $\mathbf{q}$ but different azimuthal orientations. The intensity correlation function is $g_2(q,\tau) - 1 = c_I$, where $\cdots$ indicates a time average. g_2 is related to the dynamic structure factor $f(q,\tau)$ by $g_2 - 1 = \beta f^2$, where $\beta < 1$ is a positive instrumental constant.

Fluctuations of the dynamics. To quantify dynamical heterogeneity we calculate $\chi(\tau,q)^{(\text{exp})} = \text{var}[c_I(q,t,\tau)]$, the temporal variance of the instantaneous degree of correlation $c_I(q,t,\tau)$ [24], which we correct by subtracting the contribution of measurement noise. The correction procedure is described in detail in Ref. [25]; here we simply recall its main features. The experimentally measured degree of correlation is affected by a statistical noise stemming from the finite number of pixels n_p over which this quantity is averaged. Therefore, one has [25]

$$\chi(\tau,q) = \chi^{(\text{exp})}(\tau,q) - \text{var}[n(q,t,\tau)] = \chi^{(\text{exp})}(\tau,q) - C/n_p,$$

with $\chi^{(\text{exp})}(\tau,q) = \text{var}[c_I(q,t,\tau)]$, $\chi(\tau,q)$ the desired noise-free dynamical susceptibility, $n(q,t,\tau)$ the statistical noise, and C a positive constant. The last equality stems from the central limit theorem. In order to obtain $\chi(\tau,q)$, for each q we calculate $\chi^{(\text{exp})}(\tau,q)$ by processing the same set of images with different choices of n_p (by using only 1 pixel every 1, 2, 4, 8,..., available pixels). By extrapolating the $\chi^{(\text{exp})}(\tau,q)$ vs $1/n_p$ data to $1/n_p = 0$, we obtain the desired noise free $\chi(\tau,q)$. To estimate the uncertainty associated with this procedure, we inspect the data for τ much larger than the slowest relaxation of $g_2 - 1$, where one expects $\chi(\tau,q) = 0$ [10,25]. In this limit, we indeed find $\chi = 0$ [see Figs. 2(b) and 3(b) below] within an experimental uncertainty $\sigma_\chi(q)$ which is estimated by calculating the standard deviation of $\chi(\tau,q)$ as a function of τ, at large τ. The values of $\sigma_\chi(q)$ thus obtained are taken as an estimate of the error bars on χ at all delays, and will be used in particularly in Fig. 5. The average relative uncertainty is 6% for the CB gel with $U \approx 12\ k_B T$ and less than 1% for the gel with $U \approx 30\ k_B T$.

III. RESULTS

Figure 2(a) shows $g_2 - 1$ for the CB gel with $U \approx 12\ k_B T$, at various q. The intensity correlation function exhibits a two-step decay, whose physical origin we shall discuss later. Figure 2(b) displays the τ-dependent amplitude of the noise-corrected fluctuations of the dynamics $\chi(\tau,q)$; at all q's, χ exhibits a peaked shape, strongly reminiscent of that observed in a variety of glassy systems [7,8,10,12–14,16,25,29]. The peak of the dynamical susceptibility χ^* occurs at a time delay $\tau^*(q)$ of the same order of magnitude of the decay time associated with the initial relaxation of $g_2 - 1$. Additionally, a shoulder in $\chi(\tau)$ is observed on the time scale of the final relaxation of $g_2 - 1$.

To gain insight on the physical origin of the slow dynamics, it would be desirable to quantify the decay of g_2 by fitting its relaxation by an appropriate function, such as the combination of two (stretched) exponential functions. However, due to the limited image acquisition rate, the initial decay of $g_2 - 1$ is only partially captured in our experiments, especially at the largest q vectors. As a consequence, a direct fit of the initial relaxation is not reliable. As an alternative procedure, we use a scaling analysis similar to that adopted in several photon correlation spectroscopy works (see, e.g.,

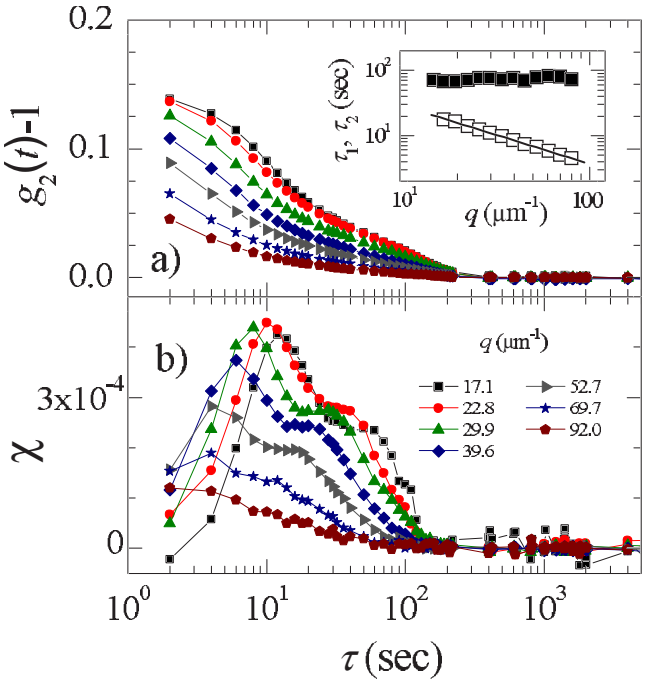

FIG. 2. (Color online) Top panel, main figure: intensity correlation functions at various q's for the CB gel with $U \approx 12\ k_BT$ (data are corrected for stray light). From top to bottom, q increases from 17.1 to 92.0μm^{-1} (see labels in bottom panel). Inset: q dependence of τ_1 (open squares) and τ_2 (solid squares). The line is a power law fit to $\tau_1(q)$ yielding an exponent -0.91 ± 0.1. Bottom panel: τ dependence of the dynamical susceptibility χ for the q vectors corresponding to those shown in the top panel. For the sake of clarity, not all available data have been plotted in the two main panels.

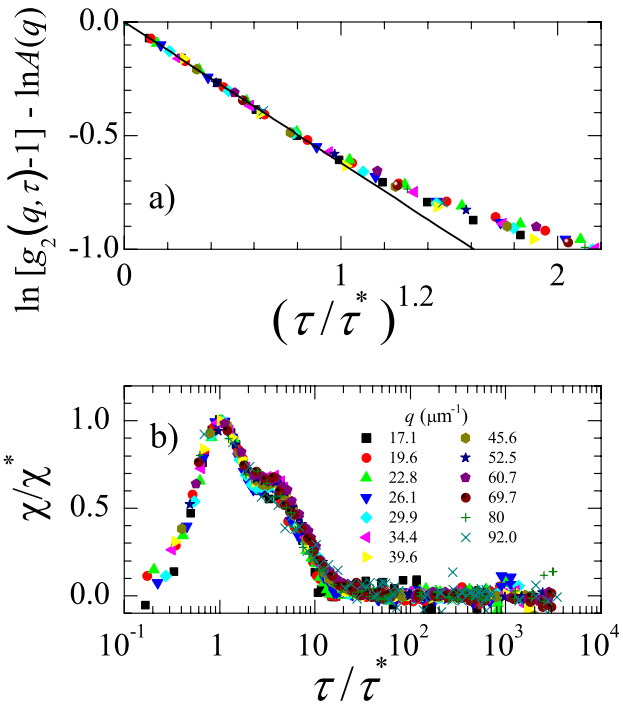

FIG. 3. (Color online) Scaling analysis of the average dynamics and of its fluctuations, for the CB gel with $U \approx 12\ k_BT$ (same data as in Fig. 2; here data at all the available q are plotted, except for the smallest and the largest, for which the data are more noisy). (a) Scaling plot of the initial decay of g_2-1. (b) Scaling plot of the dynamical susceptibility using reduced variables χ/χ^* and τ/τ^*. χ^* and τ^* are the height and the position of the peak of the dynamical susceptibility, respectively. [same symbols as in (a)].

Refs. [22,27,28], as shown for the gel with $U \approx 12\ k_BT$ in Fig. 3(a)). We first scale the lag-time axis by $\tau^*(q)$, the lag corresponding to the peak of the dynamical susceptibility χ. This choice is motivated by the fact that, quite generally, for glassy systems τ^* is of the same order of magnitude of and proportional to the system relaxation time (see, e.g., Refs. [9,29]). Furthermore, our χ data exhibit a remarkable scaling behavior, as shown in Fig. 3(b). This allows us to determine τ^* at all q with an uncertainty smaller than the temporal resolution of the CCD camera (2 s). We finalize our scaling procedure of the correlation function by normalizing g_2-1 with a q-dependent amplitude $A(q)$ which leads to a collapse of all our q-dependent data in the lag-time range of the initial decay. To determine the shape of the initial decay, we assume that the data can be modeled by a stretched exponential decay $A\exp[-(\tau/\tau_1)^{p_1}]$ and search for the stretching exponent p_1 that best linearizes our data plotted as $\ln[g_2(q,\tau)-1] - \ln A(q)$ versus $(\tau/\tau^*)^{p_1}$, where we find an optimum value of $p_1 = 1.2\pm0.2$. As shown in Fig. 3(a), a very good scaling onto a straight line is obtained for $\tau \leqslant \tau^*$; at larger lags the data curve upwards, because the initial decay of g_2 is followed by a (tilted) plateau, as seen in Fig. 2(a). The same scaling procedure is also used to characterize the initial decay for the gel with $U \approx 30\ k_BT$, for which we find $p_1 = 1.1\pm0.2$ (data not shown). Figure 4 shows some representative intensity correlation functions for both gels (symbols), together with the fits issued from the scaling analysis (lines). A full relaxation of g_2 is observed only for the gel with $U \approx 12\ k_BT$, whose final decay is well approximated by a single exponential as shown in Fig. 4(b). The fact that for the gel with $U \approx 30\ k_BT$ no final relaxation of g_2 is observed in the accessible time scale is most probably due to the deeper interparticle potential well that makes particle displacements more difficult.

The q dependence of τ_1, the characteristic time of the initial relaxation of g_2-1, is shown in the inset of Fig. 2(a) for the gel with $U \approx 12\ k_BT$. The data can be modeled by a power law $\tau_1 \sim q^{-0.91\pm0.1}$, shown in the inset of Fig. 2(a) as a continuous line (similar results are also obtained for the gel with $U \approx 30\ k_BT$). We can exclude that the initial relaxation of g_2 is due to thermally induced fluctuations of the gel branches [22], which we expect to exhibit characteristic times at least three orders of magnitude smaller than τ_1. Indeed, both the nearly q^{-1} dependence of τ_1 and $p_1 > 1$ suggest that the dynamics is determined by stress-induced rearrangements similar to those of other soft glassy materials (see Refs. [5,23], and references therein). The final decay of the correlation function is approximately exponential, with a decay time τ_2 that is q independent. This behavior most probably stems from random rare rearrangements occurring when bonds are broken, leading to particle displacements larger than $1/q$. Indeed, in this case we expect one single rearrangement to be sufficient to fully decorrelate the contri-

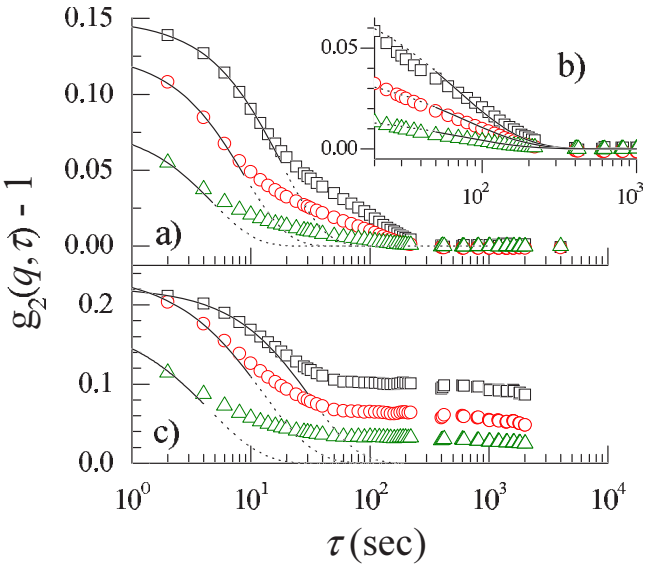

FIG. 4. (Color online) (a) Intensity correlation functions representative of the behavior at small, intermediate, and large q vectors for the CB gel with 0.2% dispersant (symbols; from top to bottom, q=17.1, 39.6, and 80.8 μm^{-1}). The lines are fits to the initial decay of g_2-1 issued from the scaling analysis described in the text. (b) Zoom on the final decay of g_2-1 for the same data as in (a), together with the large-τ fits (lines). (c) g_2-1 vs τ for the CB gel with no dispersant (symbols; from top to bottom, q=26.5, 61.2, and 141.5 μm^{-1}). In (a) and (c) the fits are represented as solid lines for $\tau \leq \tau_1$ and continued as dashed lines beyond the fitting interval.

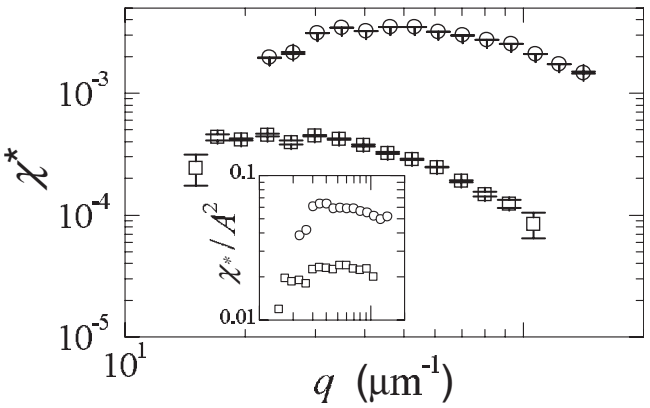

FIG. 5. Peak of the dynamic susceptibility χ^* vs q for a CB gel with 0.2% dispersant (squares) and no dispersant (circles). Error bars are calculated as explained in Sec. II. Inset: same data normalized by the squared amplitude of g_2-1.

bution of the displaced scatterers to g_2-1. The only time scale for the final relaxation of g_2 is then the average time between rearrangements, regardless of q. Assuming uncorrelated events with Poissonian statistics, one expects an exponential decay of g_2, in agreement with our measurements. As mentioned before, for the CB gel with no dispersant ($U \approx 30\ k_BT$) no final relaxation is observed within our experimentally accessible time window; this is most likely due to a decrease in the rate of bond breaking as U increases.

We investigate the length scale dependence of dynamical heterogeneity by measuring $\chi^*(q)$, the height of the peak of the dynamical susceptibility, shown in Fig. 5. For both gels, we find that $\chi^*(q)$ first increases with q, reaches a maximum value at $q \equiv q^*$ and then decreases at larger scattering vectors. Moreover, we find that the dynamical fluctuations are more pronounced for the gel with the deeper interparticle potential well. This can be intuitively understood as the size of the regions that rearrange cooperatively is presumably larger in gels with stronger interparticle interactions, leading to larger dynamical fluctuations. Additionally, it is conceivable that the relaxation process itself is more heterogeneous in time for stronger gels, where internal stress build-up and release is likely to be more important, further contributing to enhanced fluctuations. As outlined in Ref. [12], χ should in principle be normalized by the (q-dependent) squared amplitude of the relaxation of g_2-1, to allow for an explicit comparison of data obtained at different q's [26]. Here, such a correction is affected by a large uncertainty, since the short-time behavior of g_2 is barely accessible to the CCD. The height of the peak of the variance normalized using the amplitude estimated via the scaling procedure χ^*/A^2 is shown in the inset of Fig. 5. Although the data are more noisy, the peaked shape observed in the main plot is preserved.

IV. DISCUSSION

The q dependence of χ^* found here is very different from that measured in low-q light scattering experiments on strongly attractive gels made of spherical polystyrene particles [12], where $\chi^* \sim q$. One may wonder whether this discrepancy stems from a difference in the particle morphology or polydispersity. However, CB suspensions have been found to exhibit the same relaxation spectrum (as measured by rheology) as model systems consisting of spherical, nearly monodisperse colloids interacting via short-ranged depletion forces [21]. Thus, the dynamical properties reported here are likely to be generic for colloidal gels with moderate attractive interactions. Instead, we propose that the different q dependence of χ^* arises from the different q and U ranges probed in this work compared to Ref. [12]. In this section, we introduce a simple—yet general—scaling argument for the length-scale dependence of dynamical fluctuations in glassy systems that reconciles these contrasting observations. We assume the dynamics to be due to random rearrangement events each affecting a "blob" of volume V_b. The fluctuations of c_I then stem from fluctuations of $N_{\rm tot}$, the total number of events needed to decorrelate the scattered light. In determining $N_{\rm tot}$, one has to take into account that one single event may not displace particles far enough to fully suppress the local contribution to the scattered light; additionally, one single event may affect only a portion of the whole scattering volume. Thus, $N_{\rm tot} \sim N_{\rm blob} N_{\rm ev}$, where $N_{\rm blob} \sim V_{\rm sc}/V_b$ is the number of dynamically correlated blobs of volume V_b contained in the scattering volume $V_{\rm sc}$, and $N_{\rm ev}$ is the number of rearrangement events that are needed, at any given location, to relax the local contribution to the correlation function, i.e., the number of events on the time scale $\tau_{\rm r}$ of the system's relaxation. The inset of Fig. 6 is a schematic representation of this concept for $N_{\rm blob} \sim 50$ and $N_{\rm ev}$=2: in this case, g_2-1

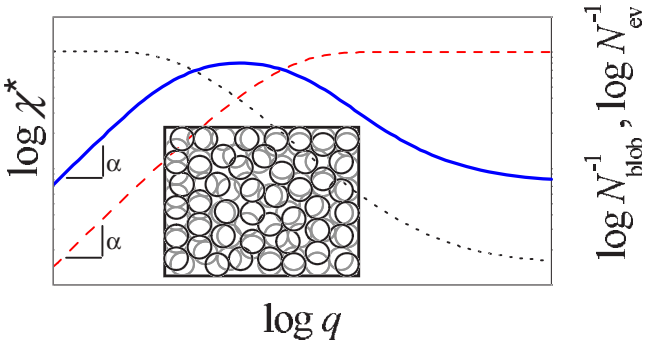

FIG. 6. (Color online) Inset: schematic representation of the rearrangement events within the scattering volume. Successive events at the same location are indicated by circles of different grey level. Main figure: qualitative double logarithmic plot of the proposed q dependence of dynamical fluctuations. Left axis: χ^* (continuous line, blue); right axis: N_{ev}^{-1} (dashed line, red), and $N_{blob}^{-1} \sim V_b$ (dotted line, black). The slope α varies between 1 and 2, depending on the nature of the dynamics, as discussed in the text.

decays to zero when at least two rearrangement events (symbolized by a black and a gray circle) have occurred at every location in the system. Given the random nature of the events, N_{tot} fluctuates, and so does c_I, with $\mathrm{var}(c_I) \sim \mathrm{var}(N_{tot})$. According to the central limit theorem, the relative variance of N_{tot}—and thus χ—is expected to scale as $N_{tot}^{-1} \sim (N_{blob}N_{ev})^{-1}$.

We stress that in general both N_{blob} and N_{ev} are q-dependent quantities. Indeed, N_{ev} decreases as q increases, because fewer events are needed to displace the particles over the smaller distances corresponding to larger scattering vectors. More specifically, in our model the average number of events is proportional to time and thus we expect $N_{ev} \sim \tau_r \sim q^{-\alpha}$. For uncorrelated particle displacements due to successive events ("Brownian-like" rearrangements), $\alpha=2$. By contrast, $\alpha=1$ if the displacement direction persists over several events ("ballisticlike" rearrangements), as found for our CB gels and other systems with internal stress-driven dynamics [5,12,23]. Note that at very large q N_{ev} should saturate to 1, when the particles' displacement due to one single event exceeds $1/q$, the length scale probed in a scattering experiment. By contrast, there are no *a priori* prescriptions on the q dependence of N_{blob}. However, it is reasonable to assume that the latter be an increasing function of q, since in glassy systems rearrangements involving displacements over large distances (probed at low q) are likely to require the highly cooperative motion of many particles, whereas smaller displacements (probed at high q) may be achieved independently by clusters containing just a few particles. Thus, for $q \to 0$, N_{blob} is expected to saturate at a lower bound, which may be as low as 1 when V_b is larger than the scattering volume, as observed in Ref. [12]. In the opposite limit $q \to \infty$, N_{blob} should saturate to N_p, the number of particles in the system.

The main panel of Fig. 6 illustrates schematically the q dependence of N_{blob}^{-1} and N_{ev}^{-1} (right axis) and that of $\chi^* \sim (N_{blob}N_{ev})^{-1}$ (left axis). At low q, $\chi^* \sim q^\alpha$, since N_{blob}^{-1} saturates to one whereas $N_{ev}^{-1} \sim q^\alpha$. This is the regime observed for the strongly attractive gels of Ref. [12], for which $N_{blob}=1$ and $\chi^* \sim N_{ev}^{-1} \sim \tau_r(q)^{-1} \sim q$ ($\alpha=1$). By contrast, χ^* tends to a constant value at very large q, because N_{blob}^{-1} saturates to N_p^{-1}, while N_{ev}^{-1} saturates to 1. The behavior of the dynamical susceptibility for intermediate q's depends on the detailed interplay between N_{blob} and N_{ev}. In Fig. 6 we have sketched the case where N_{blob}^{-1} decreases faster than N_{ev}^{-1} grows, yielding a peaked shape of χ^*, as observed in the experiments presented here.

We expect these scaling arguments to hold also for other glassy systems exhibiting dynamical fluctuations. Indeed, a growing trend in the low q regime, with $\alpha=2$, is predicted for dynamically facilitated models, for which χ^* saturates in the opposite limit $q \to \infty$ [13]. For a 2D granular system [7] and in simulations of a Lennard-Jones glass former [16] and a short-range attractive glass [15], a nonmonotonic behavior similar to that of the CB gels has been reported, with χ^* initially growing with q but then decreasing after going through a peak. The length scale corresponding to this peak is comparable to the interparticle distance for repulsive systems, while it is shifted to smaller values, corresponding to the width of the interparticle potential well, for attractive glasses [15]. Finally, the high-q regime has been explored for hard spheres within the mode coupling theory in Ref. [14], where the amplitude of χ_ϕ, a lower bound for χ_4, was reported to decrease with q around the peak of the static structure factor, in agreement with the behavior predicted by our scaling argument at large q.

Simulations of glass formers and experiments on 2D granular materials suggest that χ^* is maximum on the length scale of the particle size or that of the interparticle bond. Colloidal gels present an additional characteristic length, the size of the (fractal) clusters that compose them. For the gels of Ref. [12], χ^* was shown to grow with q for length scales intermediate between the cluster and the particle size. For the CB gels studied here, χ^* peaks at $q^* \approx 20-50\ \mu\mathrm{m}^{-1}$ (see Fig. 5), corresponding to a length scale $\Lambda \equiv 2\pi/q^* \approx 125-300$ nm, comparable to the particle size. Collectively, these observations suggest that the crossover length scale for dynamical heterogeneity in colloidal gels is of the order of or smaller than the particle size, similarly to molecular glass formers and granular materials, rather than the cluster size. Interestingly, in our gels Λ shifts towards smaller values (q^* increases) when the particles are more sticky, the same trend as that reported in Ref. [15] when going from a nearly hard-sphere system to an attractive one. Although the exact value of q^* most likely depends on the detailed shape of the interparticle potential, it is intriguing to note that the values found here ($q^*R \approx 3.6$ for $U \approx 12k_BT$ and $q^*R \approx 9$ for $U \approx 30k_BT$, respectively) are comparable to those shown in Ref. [15] for a nearly hard-sphere and attractive system ($q^*R \approx 2.5$ and $q^*R \approx 6$, respectively).

In conclusion, we have shown that the dynamics of CB gels is temporally heterogeneous. Dynamical fluctuations increase with q, peak around the inverse particle size, and decrease at larger scattering vectors. This behavior and that of other systems can be rationalized by a simple scaling argument, providing a general framework for understanding temporal fluctuations of the dynamics in glassy systems. Additionally, our measurements demonstrate that XPCS may be used to obtain quantitative information not only on the aver-

age dynamics, but also on its heterogenous behavior. This opens a new way to investigate dynamical heterogeneity in a wide variety of materials, possibly including molecular glass formers, whose characteristic length scales match those probed by XPCS, provided that a high enough signal can be collected.

ACKNOWLEDGMENTS

We thank ESRF for provision of synchrotron radiation facilities and financial support. L.C. thanks the Institut Universitaire de France for financial support. We are indebted to P. Clegg for generously providing us with some of his beam time at ESRF for control experiments. We thank L. Berthier, W. Kob and A. Duri for many useful discussions. This work was supported in part by the European MCRTN "Arrested matter" (Grant No. MRTN-CT-2003-504712), the NoE "SoftComp" (Grant No. NMP3-CT-2004-502235), the Swiss National Science Foundation, the French CNRS (PICS no. 2410), and ACI JC2076 and ANR JCJC-CHEF grants. L.C. gratefully acknowledges support of the Institut Universitaire de France.

[1] E. Donth, *The Glass Transition* (Springer, Berlin, 2001).
[2] M. D. Ediger, Annu. Rev. Phys. Chem. **51**, 99 (2000).
[3] R. Richert, J. Phys.: Condens. Matter **14**, R703 (2002).
[4] S. C. Glotzer, J. Non-Cryst. Solids **274**, 342 (2000).
[5] L. Cipelletti and L. Ramos, J. Phys.: Condens. Matter **17**, R253 (2005).
[6] E. R. Weeks, J. C. Crocker, A. C Levitt, A. Schofield, and D. A. Weitz, Science **287**, 627 (2000).
[7] O. Dauchot, G. Marty, and G. Biroli, Phys. Rev. Lett. **95**, 265701 (2005).
[8] A. S. Keys, A. R. Abate, S. C. Glotzer, and D. J. Durian, Nat. Phys. **3**, 260 (2007).
[9] L. Cipelletti, H. Bissig, V. Trappe, P. Balleta, and S. Mazoyer, J. Phys.: Condens. Matter **15**, S257 (2003).
[10] P. Mayer, H. Bissig, L. Berthier, L. Cipelletti, J. P. Garrahan, P. Sollich, and V. Trappe, Phys. Rev. Lett. **93**, 115701 (2004).
[11] R. Sarcia and P. Hebraud, Phys. Rev. E **72**, 011402 (2005).
[12] A. Duri and L. Cipelletti, Europhys. Lett. **76**, 972 (2006).
[13] D. Chandler, J. P. Garrahan, R. L. Jack, L. Maibaum, and A. C. Pan, Phys. Rev. E **74**, 051501 (2006).
[14] L. Berthier, G. Biroli, J. P. Bouchaud, W. Kob, K. Miyazaki, and D. R. Reichman, J. Chem. Phys. **126**, 184503 (2007); J. Chem. Phys. **126**, 184504 (2007).
[15] P. Charbonneau and D. R. Reichman, Phys. Rev. Lett. **99**, 135701 (2007).
[16] N. Lačević, F. W. Star, T. B. Schroder, and S. C. Glotzer, J. Chem. Phys. **119**, 7372 (2003).
[17] T. Abete, A. de Candia, E. Del Gado, A. Fierro, and A. Coniglio, Phys. Rev. Lett. **98**, 088301 (2007).
[18] V. Trappe and D. A. Weitz, Phys. Rev. Lett. **85**, 449 (2000).
[19] P. N. Pusey and W. v. Megen, J. Chem. Phys. **80**, 3513 (1984).
[20] W. B. Russel, D. A. Saville, and W. R. Schowalter, *Colloidal Dispersion* (Cambridge University Press, Cambridge, 1991).
[21] V. Prasad, V. Trappe, A. D. Dinsmore, P. N. Segre, L. Cipelletti, and D. A. Weitz, Faraday Discuss. **123**, 1 (2003); Nature (London) **411**, 772 (2001).
[22] A. H. Krall and D. A. Weitz, Phys. Rev. Lett. **80**, 778 (1998).
[23] R. Bandyopadhyay, D. Liang, J. L. Harden, and R. L Leheny, Solid State Commun. **139**, 589 (2006).
[24] Note that, contrary to χ_4 in simulations $\chi^{(\mathrm{exp})}(\tau,q)$ is not normalized with respect to N_p, the number of probed particles. For the two gels studied here, N_p is the same, because φ does not change.
[25] A. Duri, H. Bissig, V. Trappe, and L. Cipelletti, Phys. Rev. E **72**, 051401 (2005).
[26] This dependence stems from the fast dynamics at time scales shorter than those accessible to the CCD, and from the q dependence of the coherence of x-ray radiation.
[27] L. Cipelletti, S. Manley, R. C. Ball and D. A Weitz, Phys. Rev. Lett. **84**, 2275 (2000).
[28] M. Bellour, A. Knaebel, J. L. Harden, F. Lequeux, and J. P. Munch, Phys. Rev. E **67**, 031405 (2003).
[29] S. C. Glotzer, V. N. Novikov, and T. B. Schroder, J. Chem. Phys. **112**, 509 (2000).